analytical chemistry

Article

pubs.acs.org/ac

Novel Impedimetric Immunosensor for Detection of Pathogenic Bacteria *Streptococcus pyogenes* in Human Saliva

Asif Ahmed,* Jo V. Rushworth, John D. Wright, and Paul A. Millner

School of Biomedical Sciences, Faculty of Biological Sciences, University of Leeds, Leeds LS2 9JT, U.K.

Supporting Information

ABSTRACT: *Streptococcus pyogenes*, also known as group A streptococcus (GAS), is a Gram positive human pathogen responsible for invasive and noninvasive human infections with a high incidence rate. Traditional detection methods involve cell culture and PCR, which are limited by long processing times or the need for high cost equipment. Impedance-based electrochemical immunosensors provide an alternative by which precise and rapid quantitative detection of the organism can help with rapid clinical decisions. To bring a biosensor for point-of-care applications to market, strict optimization of each level of construction and operation is required. In this paper, commercial screen-printed gold electrodes have been used to construct polytyramine (Ptyr)-based immunosensors. Biotin tagged whole antibodies against *S. pyogenes* were conjugated to Ptyr amine group via biotin-NeutrAvidin coupling. Sensors were optimized at each level of construction, particularly for Ptyr electrodeposition and antibody concentration, to optimize signal and specificity. Scanning electron microscopy, fluorescence microscopy, and on-sensor analysis (HRP conjugated enhanced chemiluminescence-based semiquantitative method) to detect Ptyr surface amine and bound antibody were performed as supporting techniques. Cumulative and single shot incubations had shown detection range of 100 to 10^5 cells per 10 μL and 100 to 10^4 cells per 10 μL of bacteria in PBS, respectively. Sensors were also able to specifically detect *S. pyogenes* in 50% (v/v) human saliva, with good selectivity and low cross-reactivity.

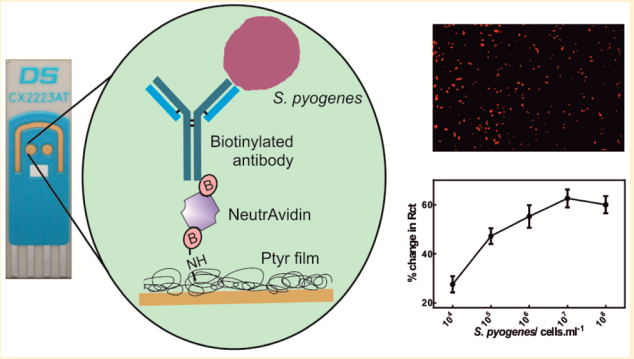

Pathogenic bacteria cause substantial mortality and morbidity worldwide. *Streptococcus pyogenes*, also known as group A *Streptococcus* (GAS), is a Gram-positive beta hemolytic bacterium, responsible for superficial and invasive disease with diverse clinical manifestations in humans.[1] Worldwide, an estimated 700 million cases of mild, noninvasive infections are reported each year of which approximately 650000 progress to serious invasive infections. The mortality rate due to invasive infection is approximately 25%.[2] In the U.K., a widespread increase in invasive GAS infections was identified in December 2010, beyond the seasonal expectation.[3]

GAS infections can be localized, invasive, and nonsuppurative postinfection sequelae (chronic inflammation without pus). They form colonies in the oropharynx and skin and have the ability to invade the epithelia causing invasive disease (e.g., bacteraemia, cellulitis, and necrotizing fasciitis). Further complications arise due to development of streptococcal toxic shock-like syndrome (STSS). Other common symptoms are abscesses, septic arthritis, and meningitis.[4] GAS strains are classified into serotypes according to their surface protein M, which is encoded by the *emm* gene. More than 200 strains have been characterized in accordance with DNA sequence variance in the *emm* gene, in a process known as *emm* typing.[5] The most frequently identified virulent invasive strain worldwide is M1, and the unusual revival of infection in the last 30 years was found to be associated with globally distributed clone M1T1. The distinguishing factors of M1T1 are bacteriophage-encoded virulence factors: extracellular streptodornase D (Sda1) and exotoxin type A (SpeA) which might have key roles in its virulence potential.[6] In general, most GAS strains show repeating emergence in a particular community at times, whereas M1T1 has shown persistence globally, both in invasive and noninvasive forms.[7]

As a safe and efficacious GAS vaccine is still to be developed, research has focused on early detection of the strain. Specific, cost-effective, and rapid point-of-care label free detection would be an advantage for faster diagnosis and better management of this disease. Most of the traditional detection methods lack these attributes as they require expensive equipment, skilled laboratory personnel, and are time-consuming. Current detection methods include culture of swabs from suspected strep throats, the beta hemolysis test, and microscopy which requires at least two days.[8] Rapid and specific commercial test strips based on latex agglutination[9] and an enzyme immunoassay[10] have been developed, but these show low sensitivity. Most of the commercial test kits are color-based strip tests and provide qualitative detection [e.g., OSOM Ultra Strep A Test

Received: October 9, 2013
Accepted: November 20, 2013
Published: November 20, 2013

(Sekisui Diagnostics), BD check Group A Strep Test (Beckton Dickinson), and QuickVue In-line Strep A Test (Quiden Corporation, San Diego, CA)].

Impedimetric sensors measure impedance, a complex parameter which includes resistance and capacitance, the result of an interaction with a small amplitude voltage signal as a function of frequency. The common formats for impedance data presentation are the Nyquist and Bode plots. In the Nyquist plot, the imaginary part of impedance (-Z″, out of phase) is plotted against the real component (Z′, in phase) at each excitation frequency. Although fabrication of impedimetric sensors can be low cost, compared to other types of sensors in terms of reproducible signal generation, they still demand further development.[11] Impedance spectroscopy has been extensively studied for a variety of analytes including small molecules,[12] proteins,[13] viruses,[14] and bacteria.[15] However, because of different electrode materials, electrode variability, different conjugation chemistries, types of analytes and different formats of data presentation, it is difficult to compare the sensitivity of different published results.

The main aim of this study was to optimize the layer-by-layer immunosensors construction on a polymer base layer using the high-affinity biotin−NeutrAvidin system (Figure 1) to target *S. pyogenes*. Here, polytyramine (Ptyr), used as the sensor base layer, was optimized to achieve a higher sensor signal. Electrochemical impedance spectroscopy was used as the main tool to investigate the sensor response, with supporting techniques including scanning electron microscopy (SEM), on-sensor blotting (an enhanced chemiluminescence-based detection method), and fluorescence microscopy. Commercially available screen-printed electrodes were used for the study to check the feasibility of translation into a commercial biosensor. Two types of analyte incubations, "cumulative incubation" of increasing concentration of bacteria on the same sensor and "single shot incubation" with different concentrations of bacteria on different sensors were also assessed to compare sensor sensitivity, as single shot incubation is considered closer to a real biosensor application scenario. The sensor successfully detected bacteria in human saliva with selectivity and low cross reactivity.

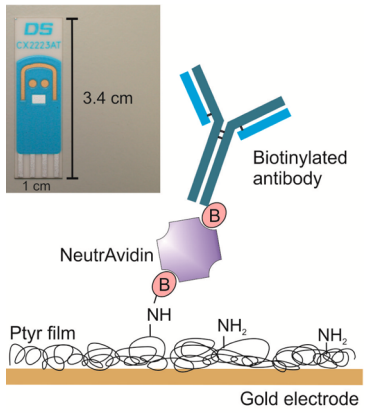

Figure 1. Schematic of immunosensor against *S. pyogenes*. Biotinyl anti-*S. pyogenes* antibodies are conjugated to the free amine of Ptyr film via biotin-NeutrAvidin bridge. The drawing is not to scale. The inset picture is a DropSens screen-printed gold electrode (CX2223AT).

EXPERIMENTAL SECTION

Materials. Horseradish peroxidase-conjugated streptavidin (streptavidin-HRP) and enhanced chemiluminescence (ECL) reagents were purchased from Thermo Fisher Scientific (Northumberland, U.K.). HRP-conjugated anti-rabbit and anti-sheep antibodies were from Sigma-Aldrich (Dorset, U.K.). Protein G purified anti-*S. pyogenes* polyclonal antibody was raised in a rabbit host against heat-inactivated *S. pyogenes* (Genescript). Anti-digoxin antibodies were raised in sheep by Therapeutic Antibodies Ltd., U.K. All other laboratory chemicals, including tyramine, (+)-biotin *N*-hydroxysuccinimide ester (NHS-biotin) were purchased from Sigma-Aldrich (Dorset, U.K.) and were of analytical grade. NeutrAvidin was purchased from Invitrogen (Paisley, U.K.). Phosphate-buffered saline (PBS; 10 mM sodium phosphate, 0.9% (w/v) NaCl, pH 7.0) was used in all experiments. Gold screen-printed electrodes (model CX223AT) were purchased from DropSens (Llanera, Asturias, Spain). Each chip has two round working electrodes, a small rectangular Ag/AgCl reference electrode and a U-shaped gold counter electrode fired onto a ceramic base.

Bacterial Culture. *Streptococcus pyogenes* (ATCC 19615) and *Streptococcus pneumoniae* bacteria were plated out onto heated blood agar (HBA) and incubated at 37 °C for 48 h. Cells were centrifuged at 3646*g* for 10 min and cell pellets were suspended in sterile PBS. Heat-killed cells were prepared by incubation at 70 °C for 2 h in a dry heat block. Successful heat killing was verified in triplicate by plating onto culture plates with no visible colonies grown. The final cell concentration of *S. pyogenes* and *S. pneumoniae* before heat killing was calculated to be 4.68×10^8 and 2.4×10^8 cells/mL, respectively.

Polymerization of Ptyr onto Electrodes. Cyclic voltammetry (CV) was employed for the electropolymerisation of tyramine, dissolved in different solvents, onto gold electrodes. Generally, tyramine was dissolved to a final concentration of 0.025 M in any of the following: 10 mM PBS, methanol, 1 M HCl, 0.5 M H_2SO_4, or methanol containing 0.3 M NaOH. Electrodes were cycled from 0 to 1.6 V using a variable scan rate and number of cycles, as mentioned in individual figure legends.

Biotinylation of Antibodies. Antibodies (5 mg mL^{-1}) were incubated with (+)-biotin *N*-hydroxysuccinimide ester (NHS-biotin; 0.2 mg mL^{-1}) in PBS under gentle agitation for 1 h. Unbound NHS-biotin was removed by three rounds of centrifugation through a 30 kDa molecular weight cutoff filter (Millipore; Billerica, MA) at 14000*g* for 2.5 min each time.

Immunosensor Construction. Polymerized electrodes were first equilibrated in PBS for 30 min before derivatization. For surface biotinylation, working electrodes were incubated with 10 μL of biotin-NHS (1 mg/mL) in PBS for 30 min, prior to washing in PBS and dH_2O and gentle drying in a stream of argon. The biotinylated surfaces were incubated with 10 μL of NeutrAvidin (diluted from stock solution of 1 mg/mL in PBS) for 45 min. This was followed by three, 5 min washes in PBS and dH_2O and drying in argon. The NeutrAvidin-functionalized surface was then incubated with biotinylated antibodies at varying concentrations for 1 h. Finally, the biosensor surfaces were washed extensively with PBS and dH_2O to remove nonspecifically bound antibodies before drying in argon. When sensors were tested in the saliva sample, after antibody immobilization, they were incubated in 1 mg/mL BSA solution to block the surface for 1 h prior washing with buffer.

dx.doi.org/10.1021/ac403253j | *Anal. Chem.* 2013, 85, 12118−12125

Characterization of Immunosensors. *Electrochemical Measurements.* Electrochemical analysis was performed in a three cell system using an EcoChemie μAutolab type III potentiostat (Metrohm Autolab B.V.; Utrecht, The Netherlands) with frequency response analyzer FRA-2. Cyclic voltammetry (CV) and electrochemical impedance spectroscopy (EIS) were carried out in an electrolyte solution of 10 mM $K_3[Fe(CN)_6]$/ $K_4[Fe(CN)_6]$ (1:1 ratio) in 10 mM PBS, pH 7.0. EIS was recorded at a 0 V potential over the frequency range from 0.25 Hz to 25 kHz with a modulation voltage of 10 mV. Autolab GPES and FRA were used to record CV and EIS data, respectively. Fully functionalized immunosensors were incubated with PBS or 50% saliva (v/v) in PBS spiked with bacteria with varying concentrations. EIS reading was taken at each layer of sensor construction and also before and after bacterial incubation. All the experiments were replicated (n = >3) with independent sensor surfaces and change in impedance after analyte addition was normalized against sensor level impedance (with no bacteria incubated). For each individual electrode, R_{ct} values were obtained from individual Nyquist plots directly using Autolab data analysis software, both at the biosensor level and at each step of analyte incubation. Then the change in R_{ct} upon incubation with a particular concentration of bacteria was calculated and normalized in percentage (with average of n = 3 or 4 as reported) using the following equation:

$$\text{Change in } R_{ct}(\%) = [R_{ct}(\text{bacteria, } X\text{concentration}) - R_{ct}(\text{biosensor})]/R_{ct}(\text{biosensor}) \times 100$$

The output files were further analyzed in statistical software Origin Pro v8 and Graphpad Prism v6.

Testing Sensor in Human Saliva Sample. Fully constructed sensors were tested in 50% (v/v) saliva in PBS. In brief, saliva samples were collected from a healthy subject in the morning after 1 h of fasting, centrifuged at 14000*g* for 5 min to pellet insoluble debris and maintained on ice.[16] Saliva was then diluted to 50% (v/v) with PBS, pH 7.0, and was spiked with either *S. pyogenes* or *S. pneumoniae* at a final concentration of 10^7 cells/mL. *S. pyogenes* were tested against sensors made with anti-*S. pyogenes* (specific) antibodies and anti-digoxin (nonspecific) antibodies to observe specific binding and cross reactivity. To test selectivity of the sensors, another GAS strain *S. pneumoniae* was tested against sensors made with anti-*S. pyogenes* antibodies.

On-Sensor Chemiluminescence Analysis of Sensor Layers. On-sensor characterization was performed at different stages of sensor construction, using targeted horseradish peroxidase conjugates followed by generation of light signal using enhanced chemiluminescence (ECL) reagent. Here, appropriate HRP-conjugated molecules can bind to a target moiety in the presence or absence of linker molecules and can generate a quantifiable light signal when imaged. In brief, to detect surface amine groups presented by Ptyr, polymer-coated electrodes were incubated in the presence or absence of biotin-NHS followed by streptavidin HRP. Biotin-NHS couples to surface amine groups to yield surface biotin moiety that can strongly bind streptavidin HRP to produce a light signal when exposed to an ECL reagent. To detect the presence of bioreceptor (full Ab raised in rabbit) on the sensor surface, HRP conjugated anti-sheep Ab or anti-rabbit Ab were incubated and a subsequent ECL signal was generated. The light signal was imaged using a G:BOX imager and further processed with image processing software ImageJ (NIH; Bethesda, Maryland). Images presented are either chemiluminescence (white light on a black background) or a superimposition of chemiluminescence on the bright-field image, where chemiluminescence has been false colored cyan to aid viewing.

Scanning Electron Microscopy. To visualize the bare electrode surface before and after polymerization, SEM was performed using a Quanta 200F (FEI) in FBS, University of Leeds. The electrodes were cut into small sizes (approximately 2 × 2 cm) and glued with carbon paste onto a 1 in. metal stub.

Fluorescence Microscopy. Bacteria bound to immunosensors were visualized using a modified protocol from Mannor et al (2010).[17] First, a stock of propidium iodide (PI) was made in dH_2O at 1 mg/mL concentration and kept at 4 °C. After the final incubation of the immunosensors with *S. pyogenes*, they were dipped in PI solution (1:500 dilution of PI stock in PBS) for 15 min. After incubation in PI, the sensors were washed with PBS and dH_2O and was imaged on an EVOS FL digital inverted fluorescence microscope. The output image was further processed in ImageJ.

RESULTS AND DISCUSSION

Electrode Preparation. Initially, DropSens screen-printed gold working electrodes were cleaned using different methods to assess their suitability for preparing electrodes for polymer deposition. Three cleaning methods used were (1) 5 min sonication of electrodes in 100% ethanol in a water bath, (2) application of 1.5 μL of piranha solution [3:7 30% (v/v) H_2O_2 and 98% (v/v) H_2SO_4] on each working electrode for 2 min (please note that piranha solution is highly corrosive and proper measures should be taken while preparing and using this solution) followed by washing with dH_2O, and (3) CV cleaning of electrodes for 15 cycles from 0.0 to 1.4 V in 0.1 M H_2SO_4 at a 50 mV/s scan rate. Impedance measurements were taken before and after each cleaning method and % changes in R_{ct} values over uncleaned electrodes were plotted (Figure S1 of the Supporting Information). It was observed that CV cleaning was the optimum cleaning method which yielded decreased R_{ct} values and a smooth surface (SEM image not shown), whereas piranha solution was not suitable as it possibly eroded and deposited dielectric material onto the working surface causing an increase in R_{ct}. However, it was observed from polymer impedance data that electrodes cleaned by sonication provided a better anchoring surface for polymers than the CV-cleaned smooth electrode surfaces. Very smooth surface derived polymers are highly capacitive in nature, whereas polymer generated upon relatively rough but clean surface, in this case sonicated electrode surfaces, gave rise to semicircular shape impedance curves with good permeability toward redox mediators (data not shown). For these reasons, despite sonication causing a small increase in R_{ct}, all electrodes were sonicated in 100% ethanol prior to polymerization to remove any loosely bound contaminants from the surface.

Optimization of Polytyramine Deposition. Different types of polymers have been used as a sensor base layer for biosensor construction, including polyaniline,[18] copolymers of aniline and its derivatives,[14] polypyrrole,[19] polytyramine,[20] and others. Each polymer has unique properties and needs extensive optimization before use in biosensor applications. There are many reported uses of Ptyr for sensor applications, including capacitive immunosensors,[21] enzyme sensors,[22] and impedance sensors.[20,23] Ptyr is reported to be very stable over a wide range

of pH and solvents in a wide potential window which makes it a good candidate for sensor applications.[24] The thickness and porosity of the polymer film can be highly controlled by different parameters, including the solvent, concentration of tyramine, CV deposition speed, and number of cycles during deposition. In this study, the Ptyr deposition was optimized with respect to its permeability toward redox mediators, so that the surface did not become overly insulating, while ensuring the presence of adequate free NH_2 groups on the surface for conjugation of bioreceptors.

It was observed from the CV pattern of Ptyr deposition (Figure S2A of the Supporting Information) that the oxidation peak observed in the first cycle does not appear in the second cycle onward, which demonstrates Ptyr's self-limiting polymerization. From the corresponding impedance data, it can be seen that as the deposition cycle increases, the impedance increases and tends to be capacitive (Figure S2B of the Supporting Information). Therefore, two scans were selected to proceed with the optimization of the CV scan speed. It was found that as scan speed increased, the impedance decreased (Figure S2C of the Supporting Information). All of the scan rates showed semicircular Nyquist plots, confirming their porous nature for redox mediator accessibility. In consideration of these facts, for sensor applications Ptyr was deposited using either a 100 or 200 mV/s scan speed, as indicated.

To further explore the effect of different solvents upon the Ptyr deposition profile, five solvents were tested. Tyramine (0.025 M) was dissolved in the following solvents: 10 mM PBS (pH 7.0), 100% methanol, 1 M HCl, 0.5 M H_2SO_4, and methanol containing 0.3 M NaOH. In all cases, two cycles were used to deposit Ptyr, using a scan rate of 100 mV/s. CV and impedance measurements were obtained for each condition. On-sensor chemiluminescent blotting was also employed to confirm the presence of available NH_2 groups on the surface. From the CV and impedance data (Figure S3, panels A and B, of the Supporting Information) of Ptyr films it was found that only methanol, in the presence or absence of NaOH, gave increased Nyquist plot semi circles, whereas both HCl and H_2SO_4 gave complex curves. The CV data corroborated these impedance recordings. The on-sensor chemiluminescence data, however, showed that although methanol-derived Ptyr had the highest Nyquist curve (largest R_{ct} value), deposition from methanol with NaOH showed maximum illumination, indicating the presence of more chemically available NH_2 groups on the surface (Figure S3C of the Supporting Information). The Ptyr film is known to display low conductivity and higher charge transfer resistance when electropolymerised in basic solution in contrast to acidic solution.[25] When the effect of NaOH concentration on Ptyr film deposited in methanol was explored with varying NaOH concentrations, it was observed that increasing concentration of NaOH conferred increasing conductivity upon the film (EIS data not shown) and also an increasing amount of surface NH_2 groups were detected by on-sensor chemiluminescence blotting. The observed increase in available NH_2 groups on the polytyramine film resulting from polymerization in basic medium with increasing NaOH may be due to an alternate polymer morphology, as dopant ions have previously been shown to influence polymerization mechanism, polymer morphology, and electrochemical properties.[26] The on-sensor blotting data highlight the fact that impedance measurements, although a useful tool for monitoring polymer deposition, do not necessarily indicate optimum polymer chemistry or information about available chemical groups on the surface. The other three solvents did not show any significant signal in the blot, so Ptyr derived from methanol containing NaOH was selected for all further experiments in the study. Figure 2A shows the CV obtained during Ptyr deposition. SEM images obtained before and after (Figure 2, panels B and C) Ptyr deposition on gold electrodes reveal the carpetlike film coating of Ptyr deposited on the gold electrode surface.

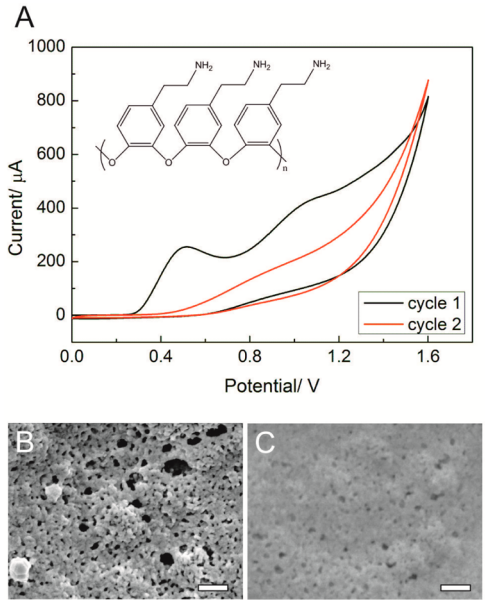

Figure 2. Electrodeposition of polytyramine. (A) Cyclic voltammogram of Ptyr deposition, 0.025 M tyramine in methanol with 0.3 M NaOH, cycled 2 cycles from 0.0 to 1.6 V at scan speed of 200 mV s^{-1}. Inset is the chemical structure of Ptyr. (B) SEM images of bare DropSens gold electrodes and (C) after deposition of Ptyr on B. The scale bars in the SEM images are 500 nm.

Optimisation of Antibody Concentration. It is very important to optimize the concentration of bioreceptors, which critically affects their conjugation onto the electrodes as well as their ease of access toward analytes with minimum physical steric hindrance. The concentration of NeutrAvidin is also important, and the use of a wide range of concentration from 6−200 μg/mL of NeutrAvidin has been reported previously to fabricate biosensors.[27] In this study, 6 μg/mL of NeutrAvidin was used unless otherwise stated.

To determine optimum antibody concentration, a wide range of antibody concentrations were incubated on Ptyr-coated sensor surfaces, keeping the NeutrAvidin concentration fixed. Then, for each antibody concentration, sensors were incubated with the same amount of analyte (*S. pyogenes* 10^6 cell/mL). The percentage changes in R_{ct} values were plotted to observe the effect of changing antibody concentration. Two controls were used; one electrode was incubated in the absence of specific antibody and another incubated with a nonspecific anti-digoxin antibody. From the raw R_{ct} values of the sensors, it was observed that as antibody concentration increased, the R_{ct} value increased, which indicates more Ab deposition on the sensor surface (Figure 3A). However, at an antibody concentration of 1 mg/mL, a slight decrease in impedance was observed, which agrees with the hypothesis that too high a density of bioreceptors can actually hinder binding because of steric hindrance at high concentration. Holford et al. (2013) showed

dx.doi.org/10.1021/ac403253j | *Anal. Chem.* 2013, 85, 12118−12125

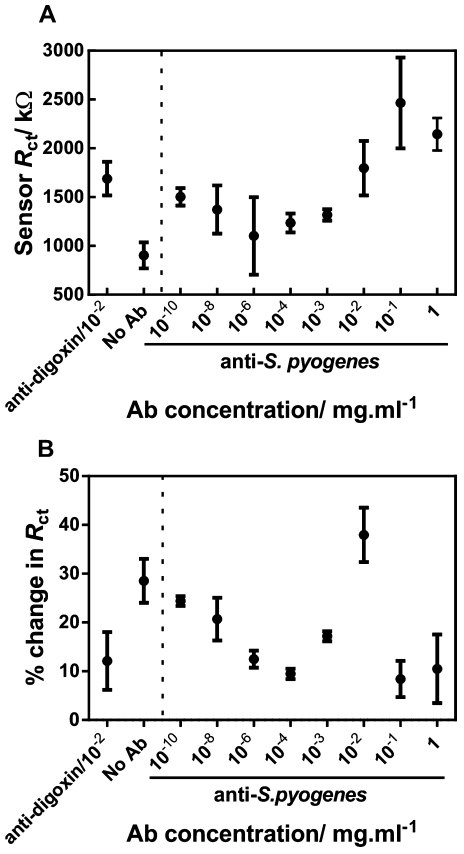

Figure 3. Antibody concentration optimization. (A) R_{ct} values of fully constructed sensors with varying Ab concentrations. NeutrAvidin concentration was kept constant at 6 μg mL^{-1}. Differences among means are statistically significant by ANOVA (**p = 0.0028). (B) Percent change in R_{ct} over biosensor after analyte (10^6 cells/mL) binding at those sensors of A. ANOVA showed differences among means are statistically significant (***p = 0.0002). All experiments are with n = 4 with SEM.

that a high concentration of antibody decreased biosensor sensitivity as it did not facilitate bioreceptor binding on the surface, probably due to steric hindrance.[27d] It was also observed that anti-digoxin and anti-*S. pyogenes* antibodies produced similar R_{ct} values (~1700 kOhm) at the same concentration (10^{-2} mg/mL). The percentage change in R_{ct} values of the above-mentioned sensors after analyte addition were plotted in Figure 3B. The R_{ct} change increased with increasing antibody concentration from 10^{-4} to 10^{-2} mg/mL. The highest sensor response was observed at an antibody concentration of 10^{-2} mg/mL but then gradually dropped above this concentration. Antibody dilution below 10^{-6} mg/mL also showed some nonspecific binding of analytes, which may be due to nonspecific *S. pyogenes* interaction with NeutrAvidin. When no antibody was present on the surface, some nonspecific binding was observed, which reduced gradually when increasing concentration of antibody was bound to the NeutrAvidin (Figure 3B, no Ab to 10^{-6} mg/mL). Again, when anti-digoxin was bound to the surface, the increased R_{ct} change observed due to the interaction with NeutrAvidin dropped significantly. From these data, the optimum concentration of antibody was selected as 10^{-2} mg/mL and used subsequently.

On-Sensor Chemiluminescent Blotting of Polymer and Fully Functionalized Sensor. Chemiluminescent blotting is a rapid and very useful technique for on-sensor surface detection. This technique employed an HRP-conjugated reagent which reacts specifically with target moieties on the sensor surface. Subsequent addition of ECL reagent generates a light signal, the strength of which is proportional to the load of target moieties on the sensor surface. The presence of primary amine groups on the Ptyr surface was confirmed by incubation in the presence or absence of biotin-NHS followed by streptavidin-HRP. A bare gold electrode was used as an additional control. Images captured after the addition of ECL reagent showed a strong signal from Ptyr deposited using a scan rate of 100 or 200 mV/s, with no signal observed in the case of bare gold and other controls (Figure 4A). The presence of

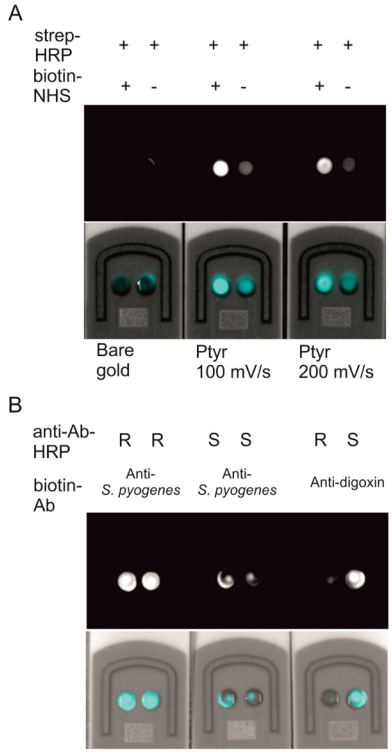

Figure 4. On sensor chemiluminescence analysis. (A) On sensor blotting for the presence of surface amines. From left to right, bare gold, Ptyr deposited at a scan rate of 100 mV/s and 200 mV/s. (B) Blot to detect the bound antibodies on surface. From left to right first two sensors conjugated with anti-*S. pyogenes* antibodies (raised in rabbit), third one with anti-digoxin antibodies (raised in sheep). R = anti-rabbit HRP antibodies, and S = anti-sheep HRP antibodies. For both A and B, the upper panels show the illumination image captured in the imager, and the lower panels are the superimposed image of electrodes and illumination signal with false cyan color.

biotinylated antibodies on the sensor surface was also detected using the same principle, with incubation in the presence or absence of appropriate HRP-conjugated secondary antibodies. Anti-*S. pyogenes* antibodies reacted with anti-rabbit HRP antibodies and anti-digoxin with anti-sheep HRP antibodies, with no or very low nonspecific reactions observed in the control electrodes (Figure 4B).

Electrochemical Impedance Spectroscopy to Detect Analyte Binding to Biosensors. Electrochemical impedance spectroscopy has been used as a sensitive and powerful technique to study sensor interfaces. The impedance of a surface can be analyzed with the complex Nyquist plot, when real and imaginary impedance components are plotted as a

dx.doi.org/10.1021/ac403253j | *Anal. Chem.* 2013, 85, 12118−12125

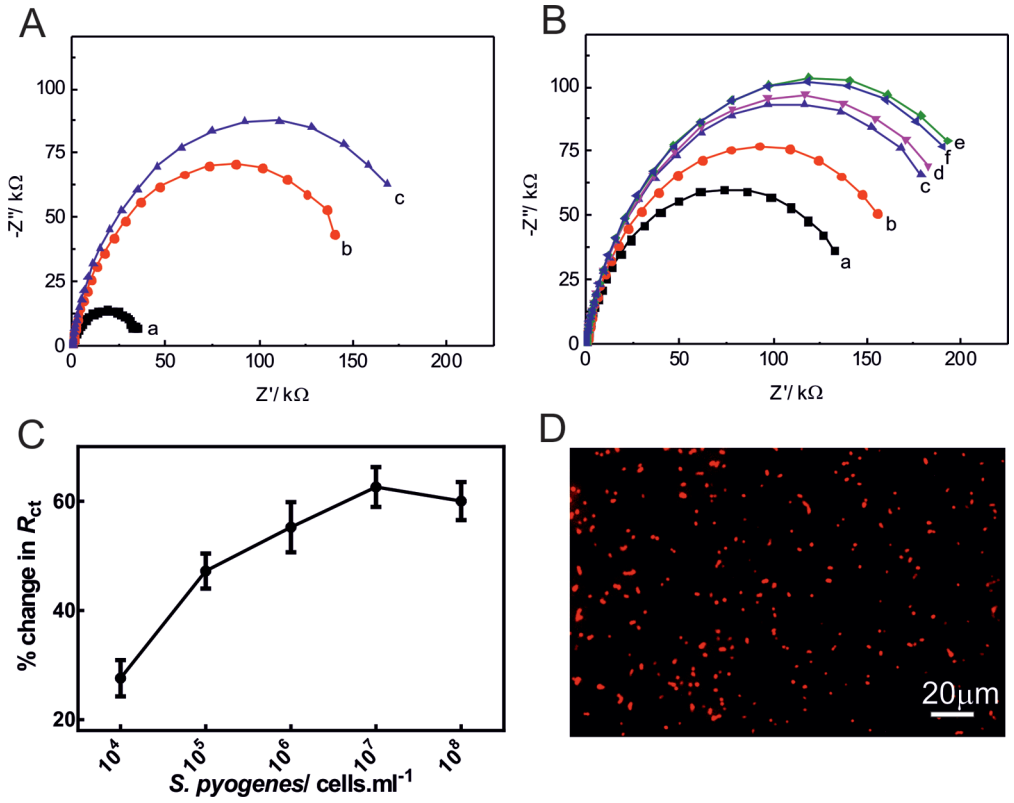

Figure 5. Immunosensor response using cumulative bacterial addition. (A) Nyquist plot showing impedance spectrum of layer-by-layer immunosensor construction, (a) Ptyr, (b) biotin-NeutrAvidin added to (a), and (c) biotinylated anti-*S.pyogenes* antibody bound to (b). (B) Impedance spectrum after addition of series of analytes to the immunosensor, (a) full-functionalized sensor, and (b–f) addition of *S. pyogenes* from 10^4 to 10^8 cells/mL. (C) Calibration curve of *S. pyogenes* immunosensor with cumulative addition of analyte; normalized data with $n = 4$ showing average ± SEM. Impedance reading was taken in 10 mM redox mediator, as described in the methods. (D) Fluorescence imaging of bound PI tagged *S. pyogenes* on the sensor surface (red dots).

function of a wide range of frequencies. Generally, an equivalent circuit model (Figure S4 of the Supporting Information) can be drawn out of the Nyquist plot to derive individual components of a sensor system [e.g., solution resistance (R_s), double layer capacitance (C_{dl}), and charge transfer resistance (R_{ct})]. During the layer-by-layer sensor construction or analyte addition, the change in R_{ct} can be measured if the experiment is performed in the presence of a redox mediator. This process is known as Faradic impedance measurement, where impedance to the redox mediator is detected due to increased deposition of material on the sensor surface. The change in R_{ct} can be normalized by calculating percentage change in R_{ct}. This can be done by calculating the percentage change of R_{ct} over immunosensors level R_{ct}. The normalization is usually useful as the raw R_{ct} values among different electrodes vary because of sensor-to-sensor variability and multiple incubation steps.

In this study, two types of incubation strategies have been employed to monitor the immunosensors response. First, cumulative or successive incubation of analytes was performed, in which the sensor was incubated in the presence of increasing concentrations of the analyte *S. pyogenes*. To achieve this, the immunosensor was incubated with the lowest analyte concentration, washed thoroughly, the impedance reading was taken, and then the next highest concentration was used for incubation. This process was repeated up to the highest analyte concentration. The R_{ct} after each step was normalized to obtain the percentage change for any particular concentration. This process was repeated using multiple electrodes to obtain the mean and SEM of data. The drawback of this approach is that when the second highest concentration is introduced, there is already some analyte bound to the sensor surface. This approach does not mirror the real application of the sensor as, in a point-of-care scenario, only a single sample is usually incubated with the sensor to obtain a reading.

As an alternative to this approach, single shot incubations have been studied, where for each concentration of analyte to be measured, a batch of three or four immunosensors was constructed. Each batch of sensors was incubated with one particular analyte concentration for 30 min, and an impedance reading was taken. The percentage R_{ct} change was calculated for each electrode to obtain a mean result. This method was applied for all concentrations of analytes. Thus, single-shot incubation provides more relevant data, considering the ultimate medical application of the device.

Cumulative Incubation. Before analyzing the analyte-binding impedance response, layer-by-layer sensor construction was monitored. Figure 5A shows Nyquist curves of the three major layers of the immunosensor. It can be clearly seen that semicircular curve increased in size as biotin-NHS and NeutrAvidin were sequentially bound to the Ptyr amine groups. The semicircle further increased in size when biotinyl anti-*S.pyogenes* were conjugated to the surface NeutrAvidin moieties. Subsequently, cumulative analyte incubation was performed using multiple electrodes and a representative Nyquist plot from a single electrode is shown in Figure 5B

dx.doi.org/10.1021/ac403253j | *Anal. Chem.* 2013, 85, 12118–12125

and corresponding equivalent circuit values are shown in Table S1 of the Supporting Information. It was observed that at the first two *S. pyogenes* concentrations, the rise in impedance was comparatively bigger than the later concentrations. This is most likely due to the decreasing availability of free antibodies after two incubations, so although the analyte concentration is high, it cannot produce as large a change in impedance. Also, the high concentration of analyte may create hindrance to itself to gain access to the antibody binding sites. It should be noted that a proportion of *S. pyogenes* cells were observed to be clustered in short chains, which also can affect antibody binding at higher concentrations. At the highest concentration, a small drop in impedance was observed, which might be due to some electron channelling to the electrodes from a surface saturated with bound bacteria. This trend was observed in many repeats, and a calibration curve with $n = 4$ was plotted (Figure 5C). An almost linear increase in % R_{ct} was observed over an analyte concentration of 10^4 to 10^7 cells/mL. It should be noted that only 10 μL of analyte solution was used which, at a concentration of 10^4 cells/mL, only contains approximately 100 bacterial cells. So, the sensor can detect bacteria in a linear range from 100 cells/10 μL up to 10^5 cells/10 μL. To confirm bacterial binding to the immunosensor, the sensor was incubated in PI solution after the final incubations and imaged under a microscope (Figure 5D). It was observed that the bound bacterial density was higher at the edges compared to the center of the electrode. This may be due to the droplet fashion incubation of the bacteria, where more bacteria tend to move toward the edges of the droplet due to surface forces. An equal distribution of bacteria was observed, where gaps between bacteria were likely due to the fact that the screen-printed electrodes have many pores and rough surface contours (Figure 2B), where antibody might not have been conjugated properly.

Single-Shot Incubation. A calibration curve derived from single shot analyte incubations was plotted, and it was observed that the linear response here was from 10^4 to 10^6 cells/mL (Figure 6A). The problem with single-shot incubations is that for higher concentration of bacteria, the access to the antibody binding sites could be limited due to steric collisions. Moreover, the droplet fashion incubation and hand pipetting reduce precision, which can be eventually overcome if robotic deposition can be performed at each stage of sensor construction to minimize electrode-to-electrode variation.

Detection of Bacteria in Human Saliva. It is always important to check sensor sensitivity and specificity in a relevant complex biological sample. Bacteria (10^7 cells/mL) spiked into a 50% (v/v) saliva sample were used to test sensor impedance response. *S. pyogenes* infection can be detected in saliva and serum, but saliva provides the ease of handling in point-of-care as the collection is invasive. *S. pyogenes* were incubated on biosensors generated using anti-*S. pyogenes* as bioreceptors to observe the change in impedance due to specific binding. *S. pyogenes* were also incubated on sensors generated using anti-digoxin (nonspecific) antibodies to check cross reactivity and a different GAS strain; *S. pneumoniae* was incubated on sensors generated with anti-*S. pyogenes* antibodies to check the selectivity of the sensors. First, all biosensors were incubated with nonspiked saliva to equilibrate the sensors and baseline impedance was recorded. Then, saliva spiked with bacteria was incubated with the corresponding sensors and changes in R_{ct} (%) were plotted (Figure 6B). *S. pyogenes* showed a very small amount of binding (4% R_{ct} change), due to cross reactivity with nonrelevant antibodies and *S. pneumoniae*

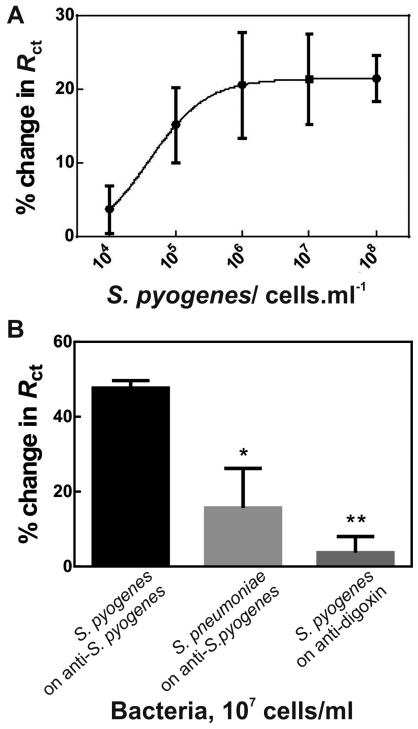

Figure 6. Immunosensors response using single incubation. (A) Calibration curve of single shot incubation. Impedance reading was taken before and after the incubation, and change in R_{ct} has been normalized to percent values. Error bars are mean ± SEM, where n = 4. (B) Sensor response in 50% human saliva (v/v) sample. First column bar shows specific binding, second and third column bars show selectivity and cross reactivity, respectively. All EIS readings were taken in 10 mM (1:1) redox mediator, as described in the methods. Error bars are mean ± SEM, where n = 3. Dunnett's multiple comparison test show statistical significance of two control panels compared to the specific panel.

displayed small signal change (16% R_{ct} change) compared to the specific binding (48% R_{ct} change), confirming the high selectivity of the biosensor. The binding observed in the latter case was likely due to *S. pneumoniae* being a closely related GAS strain that might share some epitopes that can bind to the anti-*S. pyogenes* antibodies. However, the specific signal of immunosensors is higher compared to both the control signals with statistical significance and demonstrated that the sensor can be used in complex biological samples like saliva. In addition, the use of BSA as a blocking agent for sensor surface and use of PBS containing 0.05% Tween-20 as washing buffer has helped to minimize nonspecific binding of larger bacteria onto the sensor surfaces.

■ CONCLUSIONS AND FUTURE TRENDS

In this study, biotinylated full antibody-based immunosensors have been optimized to enable the specific detection of pathogenic bacteria *S. pyogenes* in human saliva. Electrodeposited Ptyr was used as a base layer to conjugate biotinyl antibodies via a biotin-NeutrAvidin bridge. Each step of sensor construction was optimized and characterized to achieve optimum impedance response. The sensor showed linear response (100 cells/10 μL to 10^5 cells/10 μL) against *S. pyogenes* in cumulative incubation and 100 cells/10 μL to 10^4 cells/10 μL in single-shot incubation. This range covers the pathogenic load of *S. pyogenes* infection, which is around 10^6

dx.doi.org/10.1021/ac403253j | *Anal. Chem.* 2013, 85, 12118−12125

cells/mL. Sensors were also able to discriminate target bacteria in human saliva samples with low cross reactivity and high selectivity. It is likely that the performance of these immunosensors could be enhanced further through the use of oriented antibody fragments, as they are reported to be more sensitive than whole antibody-based sensors.[28] It is also considered that incorporation of robotic sensor construction[27d] will help to make sensors with a more sensitive and robust response.

■ ASSOCIATED CONTENT

Supporting Information

Additional information as noted in text. This material is available free of charge via the Internet at http://pubs.acs.org.

■ AUTHOR INFORMATION

Corresponding Author

*Address: Level 6, LIGHT Laboratories, Faculty of Biological Sciences, University of Leeds, Clarendon Way, Leeds, LS2 9JT, U.K. E-mail: bsaa@leeds.ac.uk. Tel: 00 44 113 34 37717.

Notes

The authors declare no competing financial interest.

■ ACKNOWLEDGMENTS

Asif Ahmed is funded by a University of Leeds Fully-Funded International Research Scholarship (FIRS). The authors would like to thank Dr. Vas Ponnambalam and Gareth Fearnley for support with EVOS fluorescence microscopy and Mr. Martin Fuller for his helpful training and assistance with SEM.

■ REFERENCES

(1) Cole, J. N.; Barnett, T. C.; Nizet, V.; Walker, M. J. *Nat. Rev. Microbiol.* **2011**, *9* (10), 724−736.

(2) Carapetis, J. R.; Steer, A. C.; Mulholland, E. K.; Weber, M. *Lancet Infect. Dis.* **2005**, *5* (11), 685−694.

(3) (a) *Group A Streptococcal Infections: Seasonal Activity 2010/11*; Report; Health Protection Agency: London, 2011 (b) Zakikhany, K.; Degail, M. A.; Lamagni, T.; Waight, P.; Guy, R.; Zhao, H.; Efstratiou, A.; Pebody, R.; George, R.; Ramsay, M. *Eurosurveillance* **2011**, *16* (5), 6−9. (c) Lamagni, T. L.; Darenberg, J.; Luca-Harari, B.; Siljander, T.; Efstratiou, A.; Henriques-Normark, B.; Vuopio-Varkila, J.; Bouvet, A.; Creti, R.; Ekelund, K.; Koliou, M.; Reinert, R. R.; Stathi, A.; Strakova, L.; Ungureanu, V.; Schalen, C.; Jasir, A.; Grp, S.-E. S. *J. Clin. Microbiol.* **2008**, *46* (7), 2359−2367.

(4) Cunningham, M. W. *Clin. Microbiol. Rev.* **2000**, *13* (3), 470−511.

(5) Smeesters, P. R.; McMillan, D. J.; Sriprakash, K. S. *Trends Microbiol.* **2010**, *18* (6), 275−82.

(6) Sumby, P.; Porcella, S. F.; Madrigal, A. G.; Barbian, K. D.; Virtaneva, K.; Ricklefs, S. M.; Sturdevant, D. E.; Graham, M. R.; Vuopio-Varkila, J.; Hoe, N. P.; Musser, J. M. *J. Infect. Dis.* **2005**, *192* (5), 771−782.

(7) Aziz, R. K.; Kotb, M. *Emerging Infect. Dis.* **2008**, *14* (10), 1511−1517.

(8) Steed, L. L.; Korgenski, E. K.; Daly, J. A. *J. Clin. Microbiol.* **1993**, *31* (11), 2996−3000.

(9) Gerber, M. A.; Spadaccini, L. J.; Wright, L. L.; Deutsch, L. *J. Pediatr. (N.Y., NY, U.S.)* **1984**, *105* (5), 702−705.

(10) Schwabe, L. D.; Gobbo, A. F.; Gottschall, R. L.; Randall, E. L. *Diagn. Microbiol. Infect. Dis.* **1991**, *14* (5), 367−372.

(11) Prodromidis, M. I. *Electrochim. Acta* **2010**, *55* (14), 4227−4233.

(12) Barton, A. C.; Collyer, S. D.; Davis, F.; Garifallou, G.-Z.; Tsekenis, G.; Tully, E.; O'Kennedy, R.; Gibson, T.; Millner, P. A.; Higson, S. P. J.; Labeless, A. C. *Biosens. Bioelectron.* **2009**, *24* (5), 1090−1095.

(13) (a) Ravalli, A.; dos Santos, G. P.; Ferroni, M.; Faglia, G.; Yamanaka, H.; Marrazza, G. *Sens. Actuators, B* **2013**, *179* (0), 194−200. (b) Billah, M. M.; Hodges, C. S.; Hays, H. C. W.; Millner, P. A. *Bioelectrochemistry* **2010**, *80* (1), 49−54.

(14) Caygill, R. L.; Hodges, C. S.; Holmes, J. L.; Higson, S. P. J.; Blair, G. E.; Millner, P. A. *Biosens. Bioelectron.* **2012**, *32* (1), 104−110.

(15) (a) Joung, C.-K.; Kim, H.-N.; Im, H.-C.; Kim, H.-Y.; Oh, M.-H.; Kim, Y.-R. *Sens. Actuators, B* **2012**, *161* (1), 824−831. (b) Mejri, M. B.; Baccar, H.; Ktari, T.; Aouni, M.; Abdelghani, A. *Sens. Lett.* **2011**, *9* (6), 2130−2132.

(16) Henson, B.; Wong, D. Collection, Storage, and Processing of Saliva Samples for Downstream Molecular Applications. In *Oral Biology*, Seymour, G. J.; Cullinan, M. P.; Heng, N. C. K., Eds. Humana Press: New York, 2010; Vol. *666*, pp 21−30.

(17) Mannoor, M. S.; Zhang, S. Y.; Link, A. J.; McAlpine, M. C. *Proc. Natl. Acad. Sci. U.S.A.* **2010**, *107* (45), 19207−19212.

(18) (a) Arya, S. K.; Dey, A.; Bhansali, S. *Biosens. Bioelectron.* **2011**, *28* (1), 166−173. (b) Chowdhury, A. D.; De, A.; Chaudhuri, C. R.; Bandyopadhyay, K.; Sen, P. *Sens. Actuators, B* **2012**, *171*, 916−923.

(19) Xu, Y.; Ye, X. Y.; Yang, L.; He, P. A.; Fang, Y. Z. *Electroanalysis* **2006**, *18* (15), 1471−1478.

(20) Pournaras, A. V.; Koraki, T.; Prodromidis, M. I. *Anal. Chim. Acta* **2008**, *624* (2), 301−307.

(21) Wu, Z. S.; Li, J. S.; Deng, T.; Luo, M. H.; Shen, G. L.; Yu, R. Q. *Anal. Biochem.* **2005**, *337* (2), 308−315.

(22) (a) Suprun, E. V.; Budnikov, H. C.; Evtugyn, G. A.; Brainina, K. Z. *Bioelectrochemistry* **2004**, *63* (1−2), 281−284. (b) Tsuji, I.; Eguchi, H.; Yasukouchi, K.; Unoki, M.; Taniguchi, I. *Biosens. Bioelectron.* **1990**, *5* (2), 87−101.

(23) Yang, T.; Zhou, N.; Li, Q. H.; Guan, Q.; Zhang, W.; Jiao, K. *Colloids Surf., B* **2012**, *97*, 150−154.

(24) Losic, D.; Cole, M.; Thissen, H.; Voelcker, N. H. *Surf. Sci.* **2005**, *584* (2−3), 245−257.

(25) de Castro, C. M.; Vieira, S. N.; Goncalves, R. A.; Brito-Madurro, A. G.; Madurro, J. M. *J. Mater. Sci.* **2008**, *43* (2), 475−482.

(26) Catedral, M. D.; Tapia, K. G.; Sarmago, R. V. *Sci. Diliman* **2004**, *16*, 41−46.

(27) (a) Tully, E.; Higson, S. P.; Kennedy, R. O. *Biosens. Bioelectron.* **2008**, *23* (6), 906−912. (b) Hassen, W. M.; Duplan, V.; Frost, E.; Dubowski, J. J. *Electrochim. Acta* **2011**, *56* (24), 8325−8328. (c) Hleli, S.; Martelet, C.; Abdelghani, A.; Burais, N.; Jaffrezic-Renault, N. *Sens. Actuators, B* **2006**, *113* (2), 711−717. (d) Holford, T. R. J.; Holmes, J. L.; Collyer, S. D.; Davis, F.; Higson, S. P. J. *Biosens. Bioelectron.* **2013**, *44*, 198−203.

(28) Balevicius, Z.; Ramanaviciene, A.; Baleviciute, I.; Makaraviciute, A.; Mikoliunaite, L.; Ramanavicius, A. *Sens. Actuators, B* **2011**, *160* (1), 555−562.